ISTITUTO NAZIONALE DI FISICA NUCLEARE - ISTITUTO NAZIONALE DI FISICA NUCLEARE - ISTITUTO NAZIONALE DI FISICA NUCLEARE - ISTITUTO NAZIONALE DI FISICA NUCLEARE - ISTITUTO NAZIONALE DI FISICA NUCLEARE - ISTITUTO NAZIONALE DI FISICA NUCLEARE - ISTITUTO NAZIONALE DI

Laboratori Nazionali di Frascati

Submitted to Nucl. Instr. & Meth.

LNF-90/038(P)
11 Maggio 1990

S. Bianco, F.L. Fabbri, L. Passamonti, V. Russo, A. Spallone, A. Zallo:

A STUDY OF SHORT-TERM RATE EFFECT IN PHILIPS XP-2008 PHOTOMULTIPLIER TUBES

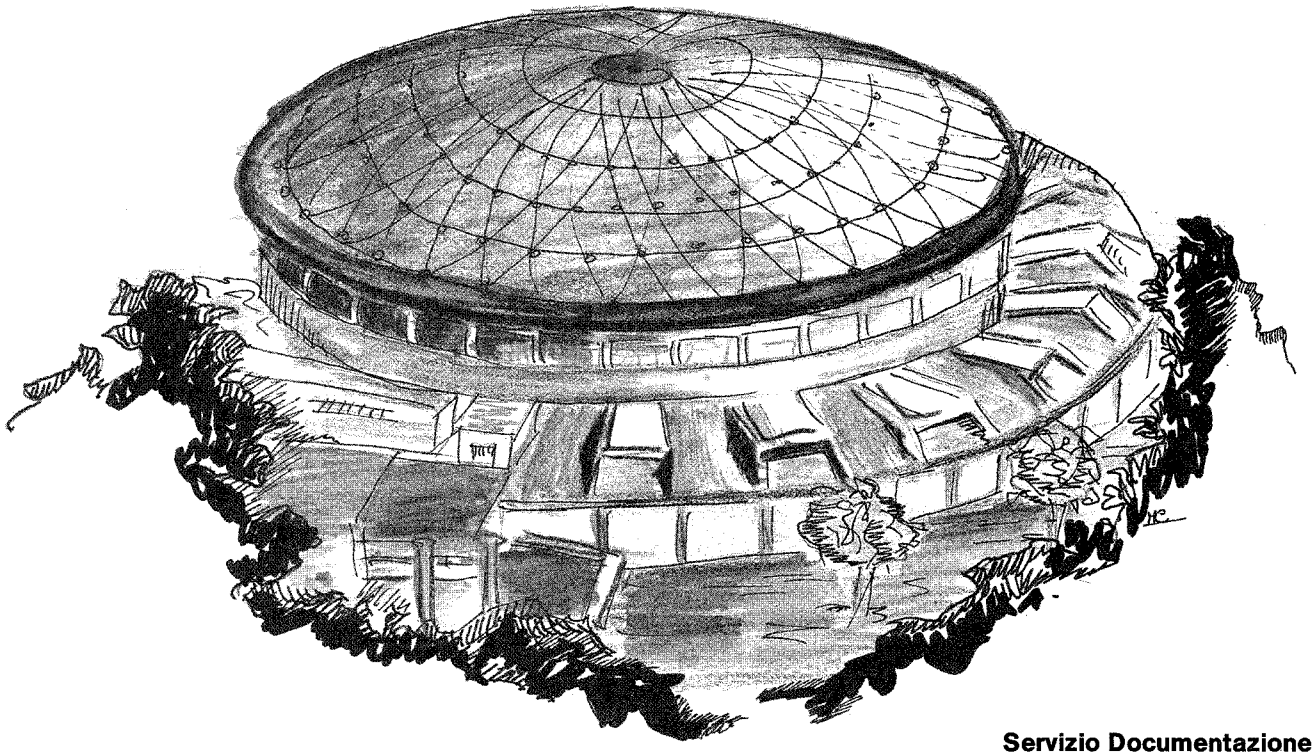

Servizio Documentazione
dei Laboratori Nazionali di Frascati
P.O. Box, 13 - 00044 Frascati (Italy)

INFN - Laboratori Nazionali di Frascati
Servizio Documentazione

LNF-90/038(P)
11 Maggio 1990

A STUDY OF SHORT-TERM RATE EFFECT IN PHILIPS XP-2008 PHOTOMULTIPLIER TUBES

S. Bianco, F.L. Fabbri, L. Passamonti
V. Russo, A. Spallone, A. Zallo

Laboratori Nazionali di Frascati dell'INFN

9 Maggio 1990
last revised: 11 Giugno 1990

ABSTRACT

A detailed study of rate effect under experimental conditions typical of accelerators is presented. Gain variations for Philips XP2008 (now available as XP2071B) photomultiplier tubes and their time dependences have been studied as functions of pulse amplitude and frequency, and tubes' high voltage supply.

1. INTRODUCTION

Photomultiplier tubes (PMT's) are widely used in High Energy Physics as light-charge transducers, for several varieties of detectors.

Requirements for suitable PMT's are a good linearity, and an excellent gain stability under every experimental conditions.

One of the major problems is due to the fact that operation at present accelerators forces PMT's to high amplitude and/or high rate light bursts: under such conditions, the gain of the PMT changes (*rate effect*), and the device is no longer linear.

Very little is known theoretically about rate effect: phenomenological models have been proposed[1], and experimental studies have been attempted[2][3][4][5]. However, due to the wide spread in PMT's behaviours under rate effect, only results on very few specimens are available, and scarce (if not none at all) data are available on the time evolution of rate effect, and its dependence on repetition rate of light pulses, anode charge, and high voltage supply. Furthermore, such measurements have been made by restricting the study to the contribution of the last dynodes, thus not providing informations on the overall sensitivity of the PMT to rate effect.

We have exploited the capabilities of a computer controlled, fully automated test system[6], to select a sample of 12 Philips XP2008 PMT's (now commercially available as XP2071B) with large gain variation characteristics, out of a total of 276 from the wide-angle em calorimeter of the NA1 experiment at CERN.

On such a sample we have performed a systematic study of gain variations, and of their time dependences, due to the whole PMT; these quantities have been studied as functions of total anode charge, repetition rate, and high voltage supply.

2. THE APPARATUS

The XP2008 is a ten-stage photomultiplier, with a semitransparent $SbCs$ photocathode; the dynode structure is linearly focused, with $CuBe$ dynodes. The maximum high voltage allowed is $1800\,V$, the maximum mean anode current is $200\,\mu A$ with the voltage divider adopted, and the maximum peak anode current is $200\,mA$.

The experimental apparatus (fig.1) is composed of a box containing 12 PMT's optically coupled to the LED's light source, a HV power supply, a LED pulse generator, trigger logic and read-out electronics.

The box and the room are independently conditioned: the environmental temperature is kept constant within $\pm 1^\circ C$, while the temperature in the box is stable within $\pm 0.5^\circ C$. An electronic thermometer monitors the temperature in the box, and its output is digitized and sent to the ADC.

PMT's and LED's are powered by a CAMAC-compatible voltage supply[7], with a precision of $\pm 0.2\%$.

A 10-dynode voltage divider with grounded-anode is used (fig.2). Voltage drops increase starting from the $4th$ stage: this arrangement provides a better gain linearity, since the stronger field between the last dynodes raises the threshold electronic current at which

the space charge saturation is established. The current flowing in the divider is $I_d = 1.6mA$ at $-1600\,V$.

The pulse generator FRAM77[8] flashes a set of HP5082-4956 green LED's, emitting at a wavelength $\lambda = 565nm$. Typical rise time of pulses is $\sim 2ns$, the $FWHM \sim 2ns$ and the fall time is $3 \sim 4\,ns$. The LED's output has a risetime $\sim 5ns$ and a fall time $\sim 50ns$: this is a realistic simulation of the light pulses in organic scintillators, when the signal travels through cable lengths typical of High Energy Physics experiments (*i.e.*, $100m$ of a RG58 type cable).

LED's are assembled outside the box housing the PMT's, and are matched to the photocathodes by quartz optical fibers.

Two different bunches of LED's are used. The former bunch ("RLED") is continuously pulsed at low frequency ($\nu_R \sim 100\ Hz$), therefore supplying a very low mean anode current $I_R = Q_R \cdot \nu_R$, with Q_R being the anodic charge associated to each RLED light pulse: it allows to monitor PMT's gain before, during, and after the high current burst. The latter bunch ("BLED") is used to simulate light bursts on the PMT photocathode, thus reproducing the operation at pulsed accelerators. The PMT mean anode current during the burst ($I = I_R + I_B$) can be varied by changing the frequency ν_B and/or the number of photoelectrons N_B of the light pulses from the BLED. This allows to perform measurements at various N_B and ν_B, in order to disentangle frequency and peak current effects, for a fixed mean anode current. Special attention was paid, to avoid fixed phases between RLED and BLED light pulses in all measurements performed.

This arrangement employing two sets of LED's makes all gain measurements independent on variations of LED's output, possibly due to the sudden change in frequency and/or pulses amplitude.

While the RLED bunch emits light pulses corresponding to about 300 photoelectrons, the BLED can emit light pulses in the range $10^3 \div 10^5$ photoelectrons. The pulse generator FRAM 77 allows to vary the frequency of the BLED pulses from $128\,Hz$ to $32768\,Hz$.

The acquisition system (fig.3) enables an ADC gate for each RLED pulse, unless a contemporaneous BLED pulse occurs.

The anode charge is measured by 11-bit LRS-2249W Analog-to-Digital Converters: the conversion slope is $0.250\,pC/channel$, and the maximum integral deviation from linearity is better than 0.25%.

The system stability is monitored by a reference PMT optically coupled to the RLED only, and kept at constant HV supply: the long-term gain stability over the test period was better than 2%.

A CAVIAR microcomputer[9] is used for DAQ, on-line monitor and measurements management. It is based on the 6800 8-bits processor, and is provided with CAMAC and graphic software. An IEEE-488 interface controls a line printer and a 5"1/4 floppy-disc; an RS-232 interface and a data communication protocol allow to link CAVIAR to a host computer (in our case a $VAX\,11/780$).

3. SHORT-TERM GAIN VARIATIONS

We have extensively studied rate effect for 12 XP2008 PMT's at a high voltage supply of $-1680V$, namely 80% of the maximum allowed by the manufacturer.

Some tests were also done with PMT's supplied at lower and higher voltages, to study the influence of a change in the HV supply on rate effect.

Gain variations have been measured with respect to a reference state, in which one light pulse from the RLED corresponds to $N_R \sim 300$ photoelectrons, and the count rate is $\nu_R = 100\,Hz$. Such light pulses correspond approximately to those due to a minimum ionising particle, crossing $1\,cm$ of NE102 scintillator. We have checked the effect of changing ν_R and Q_R within a factor $2 \sim 3$ to obtain the same I_R, with no difference on PMT's gain. We shall indicate as G_0 ($\sim 10^6$) the PMT gain in this reference state.

We have studied gain variations between this reference low current state, and several states that we characterise by the expected mean anode current in absence of rate-related gain variations $I = I_R + I_B$, where $I_B = e \cdot N_B \cdot G_0 \cdot \nu_B$.

The maximum *burst* mean anode current provided by the BLED ($I = 80\,\mu A$) is well below the maximum allowed by the manufacturer ($I_{max} = 200\,\mu A$), and still much lower than the current flowing in the voltage divider. Nevertheless, to check the presence of problems related to a redistribution of inter-dynodes potentials, we have repeated all measurements on one PMT, supplying the voltage to the last two dynodes by means of an external high-current power supply. No difference was found in the whole range of measurements up to ($I = 80\,\mu A$) and to a voltage of $-1800\,V$ between those 2 HV supply configurations.

To study the rate effect in realistic conditions, we simulated a cycle similar to the experimental conditions at present accelerators, in which particles are spilled during a few-seconds burst, followed by an idle period. We define as "short-term" rate effect, the gain variation observed in such cycles: the cycle chosen is composed of a $10\,s$ burst, followed by a $50\,s$ recovery time.

When light amplitude and/or rate on the photocathode are raised, PMT's gain increases exponentially with time, reaching a new stable value after few tenths of a second. The gain stays stable during the high-current burst, and an exponential recovery is observed when the excitation is turned off at the end of the burst (fig.4).

Since typical times to be measured (i.e. those necessary to reach and leave the excited state) are much faster than the time necessary to acquire 1 event, and to transfer it on to mass memory, we have used a sampling technique. This is required by the fact that the DAQ system run by CAVIAR needs more than $500\,ms$ between two ADC readings, to transfer the data to mass memory (*i.e.* VAX 11/780 or floppy-disc). To overcome this bound, we sampled the $10\,s$ period several times, shifting each time a hardware-generated delay. A circuit (shown in fig.5) allows to delay from 50 to $500\,ms$ the external trigger driving the BLED; read-out of the ADC immediately after both start and end of the high-current burst is thus possible. Measurements collected are superimposed in the off-line analysis, and the final curve $\Delta G\,vs\,t$ is obtained (fig.6).

The gain variation is defined as

$$\Delta G = \frac{< ADC - PED > - < ADC_0 - PED_0 >}{< ADC_0 - PED_0 >},$$

where ADC_0 and PED_0 are the output signal and pedestal values of the RLED light pulse at the reference state ($I = I_R$), and ADC, PED are the same quantities during the high-current burst. Pedestals are measured in dedicated runs in order to correct for frequency-dependent pedestals shifts.

The gain variation has been investigated at various mean anode currents

$$I \simeq Q_B \cdot \nu_B$$

for different combinations of charges Q_B, and pulse frequencies ν_B.

The raise of PMT's gain to the excited level ΔG_{max} is represented by the time dependence

$$\Delta G(t) = \Delta G_{max} \cdot (1 - e^{-\frac{t}{\tau_e}}). \qquad (3.1)$$

Similarly, at the end of the burst, the original level is reached with a time dependence

$$\Delta G(t) = \Delta G_{max} \cdot e^{-\frac{t}{\tau_r}}. \qquad (3.2)$$

Quantities ΔG_{max}, τ_e and τ_r have been measured as functions of I, at 5 different values of Q_B,

$$Q_B = n \cdot (Q_B)_0 \qquad n = 1,5.$$

The anode charge $(Q_B)_0$ is due to $N_B \sim 10^4$ photoelectrons, and corresponds to about $2500\,pC$ in absence of rate effect, keeping the high voltage at $HV = -1680\,V$.

For each specimen, the gain variation ΔG_{max} appears to be independent on how Q_B and ν_B are combined to form the same I, within the experimental errors (fig.7). Therefore, ΔG_{max} is parametrized as a function of I only, by the law

$$\Delta G_{max} = p_1 \cdot I^{p_2}. \qquad (3.3)$$

Parameters p_1 and p_2 are computed by means of the best fit of the experimental points: fig.8 shows their distributions for the sample of 12 PMT's tested. We find for our sample of 12 PMT's values for exponents $0.4 \leq p_2 \leq 0.7$.

Excitation and relaxation times τ_r, τ_e are plotted as functions of I and Q_B in figg.9,10, showing a decrease when I is increased; furthermore, a dependence on Q_B is also evident, as high Q_B correspond to low $\tau_{r,e}$. The dependence of $\tau_{e,r}$ on I and Q_B is well approximated by the law

$$\tau_{e,r} = \frac{b_{e,r}}{I^{c_{e,r}}} \qquad (3.4)$$

Fig.11 shows the distribution of the parameters $b_{e,r}$ and $c_{e,r}$ obtained from the best fit of (3.4) to the data. Scale coefficients $b_{e,r}$ show a similar inverse proportionality on Q_B, while

exponents $c_{e,r}$ do not depend on Q_B. Fig.12 shows the correlation between parameters b, c in (3.4).

Measurements have been repeated for 3 different values of the high voltage supply $HV = -900, -1680, -1800\,V$, keeping the anode charge constant $[Q_B = 3(Q_B)_0]$.

A slight dependence of ΔG_{max} on HV has been found; the variation is $\sim 5\%$ at $80\mu A$ between $-900\,V$ and $-1800\,V$ (fig.13). A dependence has also been found for $\tau_{e,r}$: the time necessary to reach (and to leave) the excited state characterized by ΔG_{max}, diminishes for higher supply voltages (figg.14,15).

By the measurements illustrated so far we have investigated the overall rate effect, *i.e.* that due to the sum of gain variations from all amplification stages.

Nevertheless, some authors[4] claim rate effect should be explained as due mainly to the last dynode, through an enhanced conductivity mechanism.

To isolate the contribution of the last *(10th)* dynode to the overall gain variation, we have used a subtraction method.

Both voltage divider and read-out circuitry were modified by supplying the anode with the same voltage than the 10th dynode, leaving all remaining voltage drops unchanged. In this configuration the PMT acts as a 9-dynode device, and gain variations due to the 10th dynode $(\Delta G_{max})_{10}$ are isolated comparing results in both supply schemes:

$$(\Delta G_{max})_{10} = \Delta G_{max} - (\Delta G_{max})_{1\div 9}.$$

Fig.16 shows the separate contributions to the gain variation of the whole multiplicative chain, and of the last stage only.

Such measurements have been done at HV supplies corresponding to cathode-anode voltage drops of $-900\,V$ and $-1800\,V$ respectively, in the 10-dynode configuration.

The last dynode appears to account for only about 20% of the total gain variation: we find indeed

$$\Delta G_{max} : (\Delta G_{max})_{1\div 9} = 1 : 0.8.$$

4. CONCLUDING REMARKS

We have extensively studied a relevant sample of XP2008 PMT's, determining their most significant parameters in rate effect conditions. Rate effect has been studied under experimental conditions typical of particle accelerators, with on-off structures in the seconds domain*(short-term rate effect)*.

We have shown that the gain variation is a function of the average anode current in the PMT, and does not depend separately nor on the amplitude nor on the frequency of light pulses impinging on the photocathode. All stages in the PMT's multiplicative chain contribute similarly to the overall effect. We do not observe any magnification of the effect at the last dynode.

Transition times to the new "excited" working state, and from there back to ordinary conditions, depend inversely on both the amplitude of light pulses on the photocathode (*i.e.* the anode charge), and the mean current flowing in the PMT. An analytical relationship has been found between transition times and those two quantities (3.4).

Provided the mean current is kept constant, we also found that while the gain variation is practically independent on the operating HV, there is an inverse relationship between transition times and voltage supply applied.

Only one paper[3] has been published on the same PMT model, but confined to a limited set of measurements, and besides investigating only one specimen. To make a comparison of global trends, only a few articles are available concerning similar PMT's studied under short-time rate effect. We report in Tab.I a compilation of available data compared with ours.

General agreement is found in the literature on gain variations as not depending separately on the pulse frequency and amplitude, but only on their product. Gain variations are directly proportional to the anode current: absolute values for samples studied in the literature are quite different from PMT to PMT, ranging from $\sim 10\%$ to $\sim 60\%$ at a mean anode current of $\sim 50\,\mu A$.

We found the dependence of the gain variation on the average anode current well represented by a power-log law, with exponent in the range $0.4 - 0.7$, depending on the specimen. This parameter seems to be fairly well reproduced by all available measurements, considering the wide range of characteristics for the PMT's studied.

A quantitative comparison with the only other result on XP2008[3] is difficult, since no description is given therein on what on/off cycle was used. Nevertheless, when we parametrise their data as functions of the mean anode current, the gain variation can be described as well by a power-log law, with exponent $p_2 \sim 0.6$.

Data has been published previously[2][4][5] on the time necessary for the PMT's gain to reach and leave the new state, at the beginning and end of the light burst. We found such times to be inversely correlated to the anode current, namely high current correspond to fast times. Moreover we pointed out that, for a given anode current, transition times

are shorter when the amplitude of the light pulse is bigger. A similar behaviour has been shown in ref.[5] on FEU PMT's. However, an early study[2] on FEU PMT's claimed that a correlation similar to ours exists only for excitation times, but not for relaxation times.

Authors in ref.[4] have found a behaviour qualitatively comparable to ours, however isolating the contribution due to the last dynode only. Quantitative comparison is thus not possible.

Finally, our results on the relative contributions of different amplification stages to rate effect show that the gain variation due to the multiplicative chain with the last dynode excluded is approximately in the ratio 0.8 : 1 when compared to the gain variation due to the whole chain. Substancial agreement is found with ref.[5], claiming a ratio 0.9 : 1.

These results suggest that the last dynode is not the main contribution to the phenomena, as often claimed in the literature, but instead all dynodes contribute with a comparable effect. Surprisingly, disagreement is found on this issue with ref.[4] on XP2030 PMT's. The relative contribution found is about 0.3 : 1. The authors explained this result with an electron enhanced conductivity of the dynodic oxyde surface model, which predicts a larger effect on the last dynode, where a larger number of electrons are extracted. Such a model is not adequate to describe our data, and suggests that the mechanism could be more complicated.

Comparison between the results presented in this paper and the available data in literature shows that, whilst a general agreement is found for what concerns the qualitative aspects of the rate effect phenomenology in pulsed regime, it is not possible to describe all results within a general model yet.

Moreover, the influence of the specific on-off cycle adopted needs to be further clarified, in order to allow both a meaningful comparison between various authors' measurements, and a general way of relating the PMT's behaviour under rate effect conditions to the manufacturer's specifications.

ACKNOWLEDGEMENTS

We gratefully acknowledge the contribution of L. Daniello and M. Giardoni, whose technical skills made the PMT's test apparatus possible.

REFERENCES

[1] I. Cantarell and L. Almodóvar, Nucl. Instr. and Meth. **24** (1963) 353.

[2] G. A. Akopdzhanov *et al.*, Nucl. Instr. and Meth. **161** (1979) 247

[3] F. Celani *et al.*, Nucl. Instr. and Meth. **190** (1981) 71.

[4] M. De Vincenzi *et al.*, Nucl. Instr. and Meth. **225** (1984) 104.

[5] V. N. Evdokimov and M. I. Mutafyan, Instr. Exp. Tech. **29** (1986) 900.

[6] S.Bianco *at al.*, A COMPUTER CONTROLLED SYSTEM FOR TESTING LARGE QUANTITIES OF PHOTOMULTIPLIER TUBES, INFN Frascati LNF-85/49(R).

[7] G. Bologna *et al.*, Nucl. Instr. and Meth. **192** (1982) 315.

[8] R. Baldini-Celio *et al.*, Nucl. Instr. and Meth. **180** (1981) 249.

[9] S. Cittolin and B.G. Taylor, CAVIAR User Manual, DD/OC/GA/80-2.

[10] M. Bonesini *et al.*, Nucl. Instr. and Meth. **A264** (1988) 205.

Tab. I Compilation of data on short term rate effect. Columns 5 to 10 show the qualitative behaviour of transition times when mean anode currents, anode charges and HV are increased. Transition times are found decreasing (⇓) or not depending (ND) on those quantities.

Ref.	PMT model	n PMT's	P2	$\tau_e(I)$	$\tau_r(I)$	$\tau_e(Q_a)$	$\tau_r(Q_a)$	$\tau_e(HV)$	$\tau_r(HV)$	$(\Delta G)_{1\div 9} : \Delta G$
[2]	FEU-84 FEU-85 FEU-110 FEU-115 XP2010	32 16 3 16 1	1 "linear"	⇓	ND					
[3]	XP2008	1	0.6							
[4]	XP2030	1	0.5-0.7	⇓	⇓	⇓	⇓	⇓	⇓	0.3:1
[5]	FEU-49B FEU-84-3	1 1	0.3 0.6	⇓	⇓					0.97:1 0.9:1
[10]	XP2972	3456	0.7							
this paper	XP2008	12	0.4-0.7	⇓	⇓	⇓	⇓	⇓	⇓	0.8:1

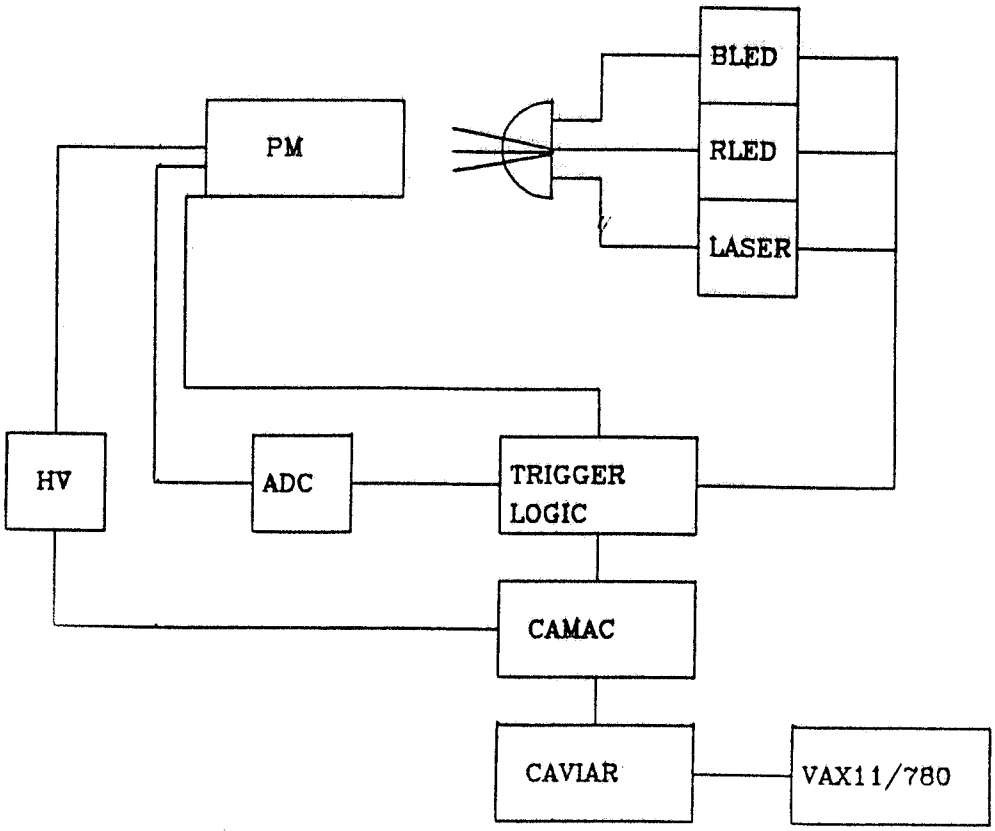

Fig. 1 The experimental apparatus used for the tests.

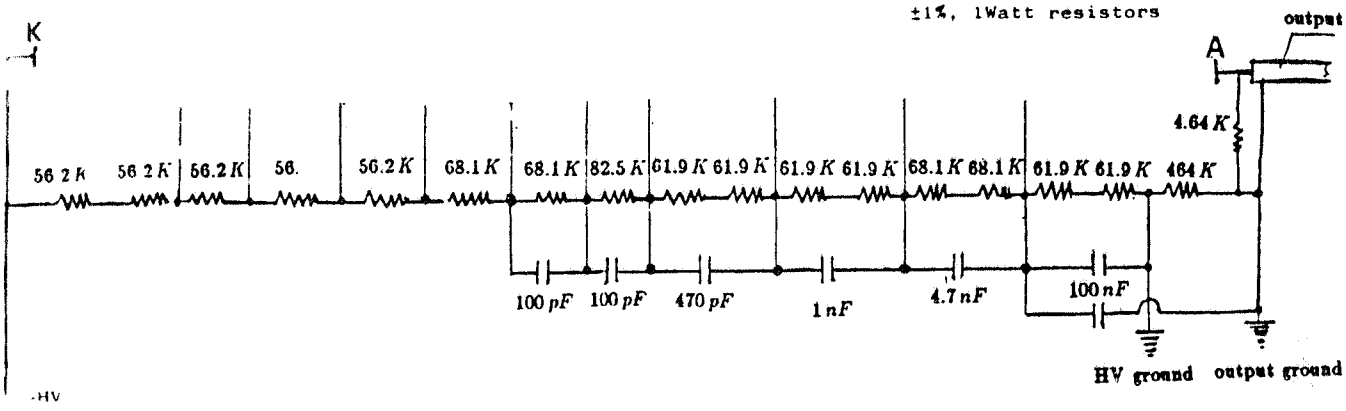

Fig. 2 The high-linearity voltage divider.

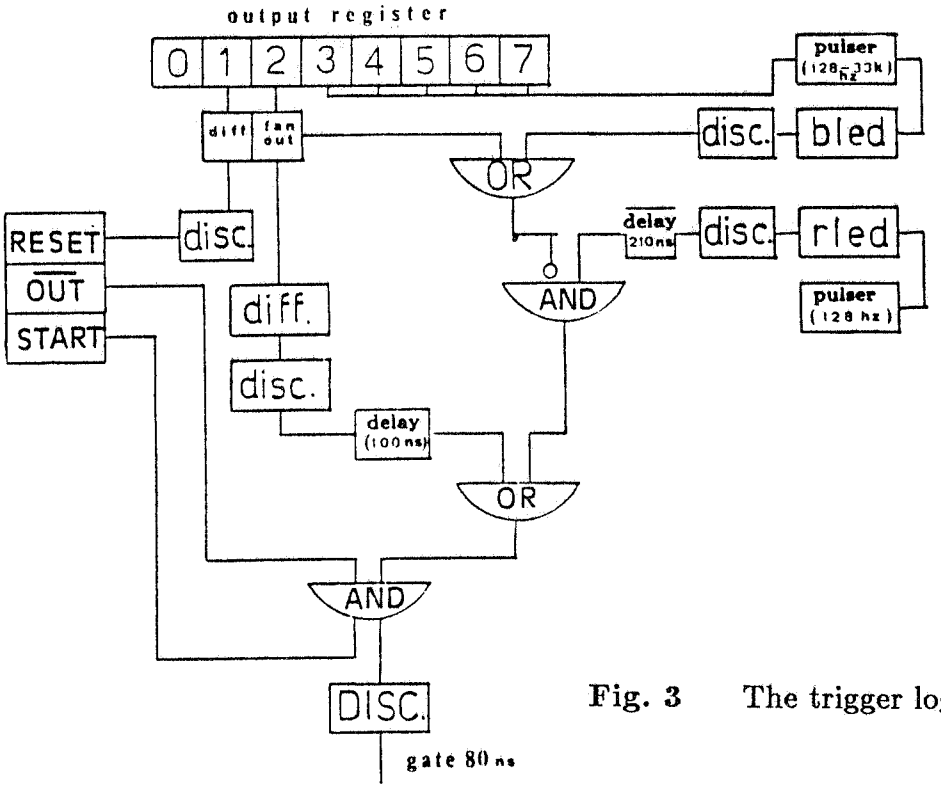

Fig. 3 The trigger logic.

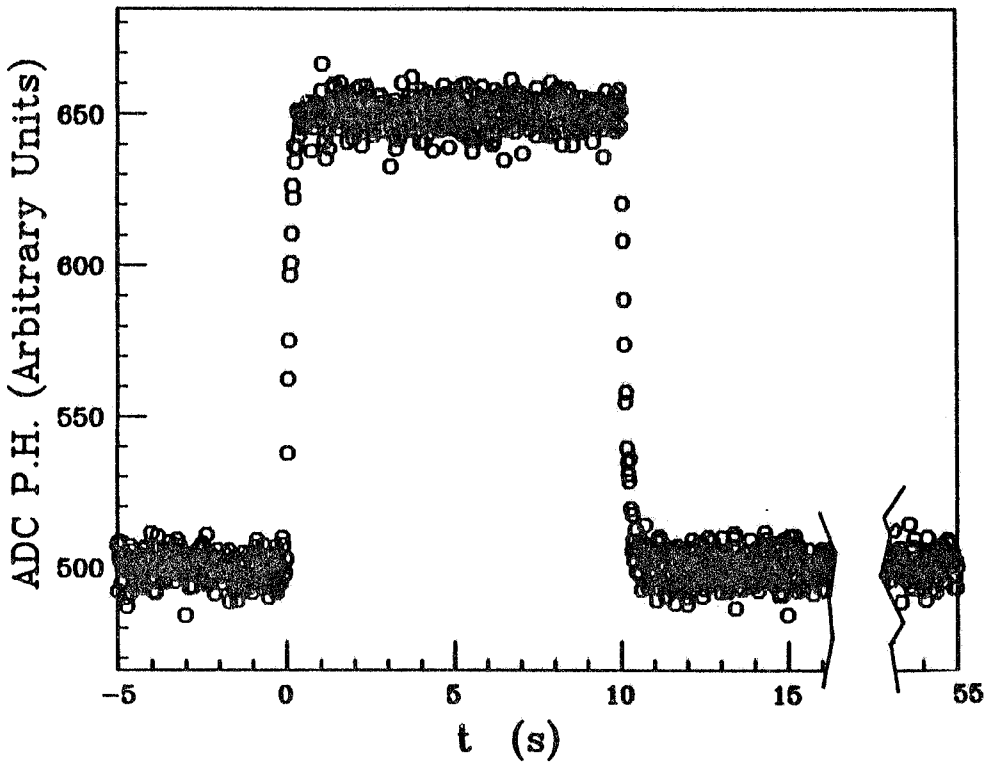

Fig. 4 A typical example of PMT gain behaviour during the cycle adopted.

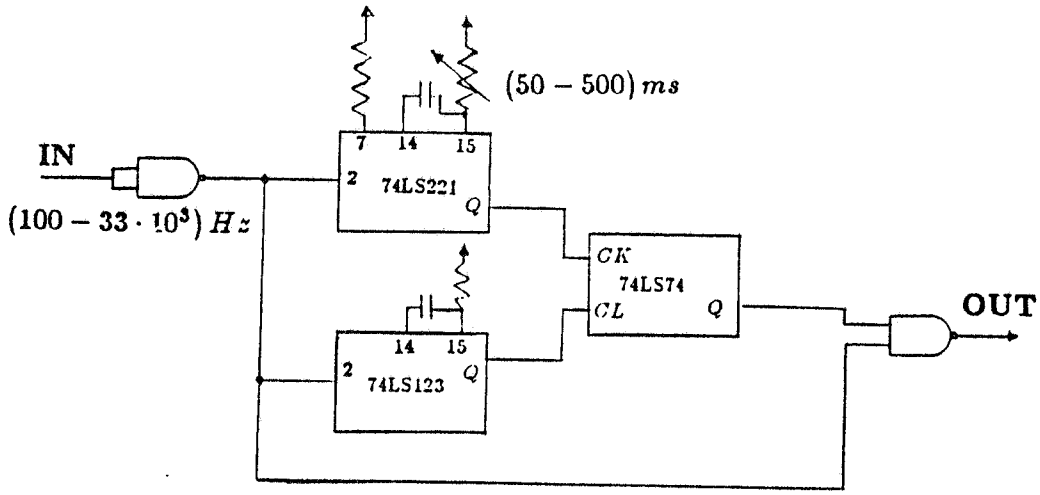

Fig. 5 Variable delay circuit permitting the time-shift mechanism.

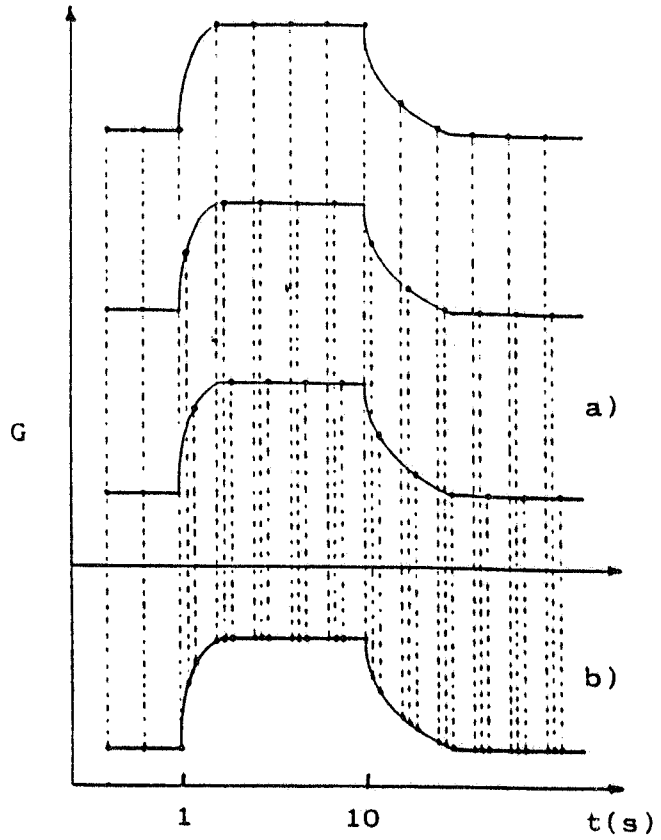

Fig. 6 Time-shift mechanism in the excitation cycle for short term rate effect. Measurements are iterated by setting an increasing delay each time [6a)]. The final gain variation is obtained by overlap of every measurement [6b)].

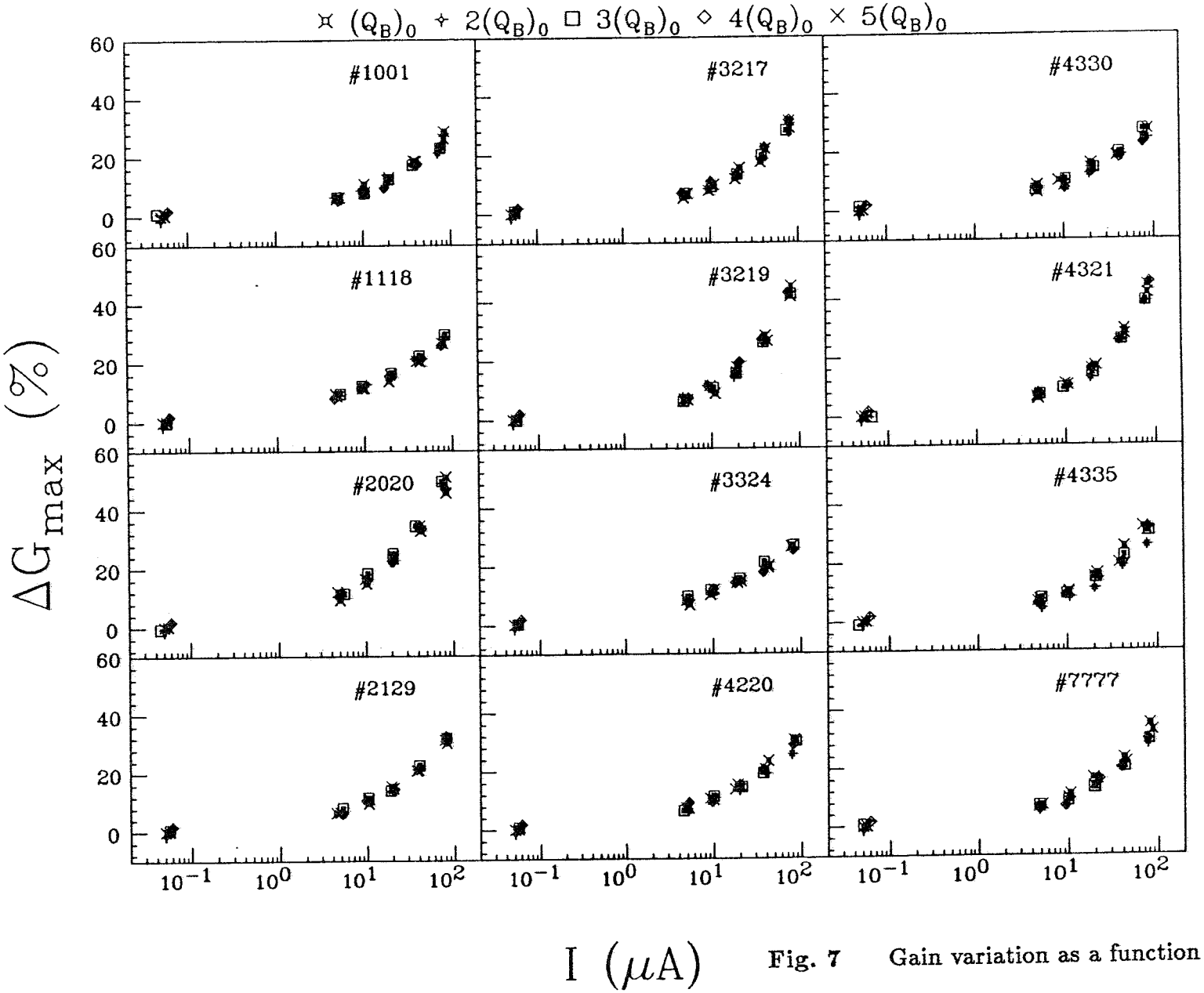

Fig. 7 Gain variation as a function of I and Q_B.

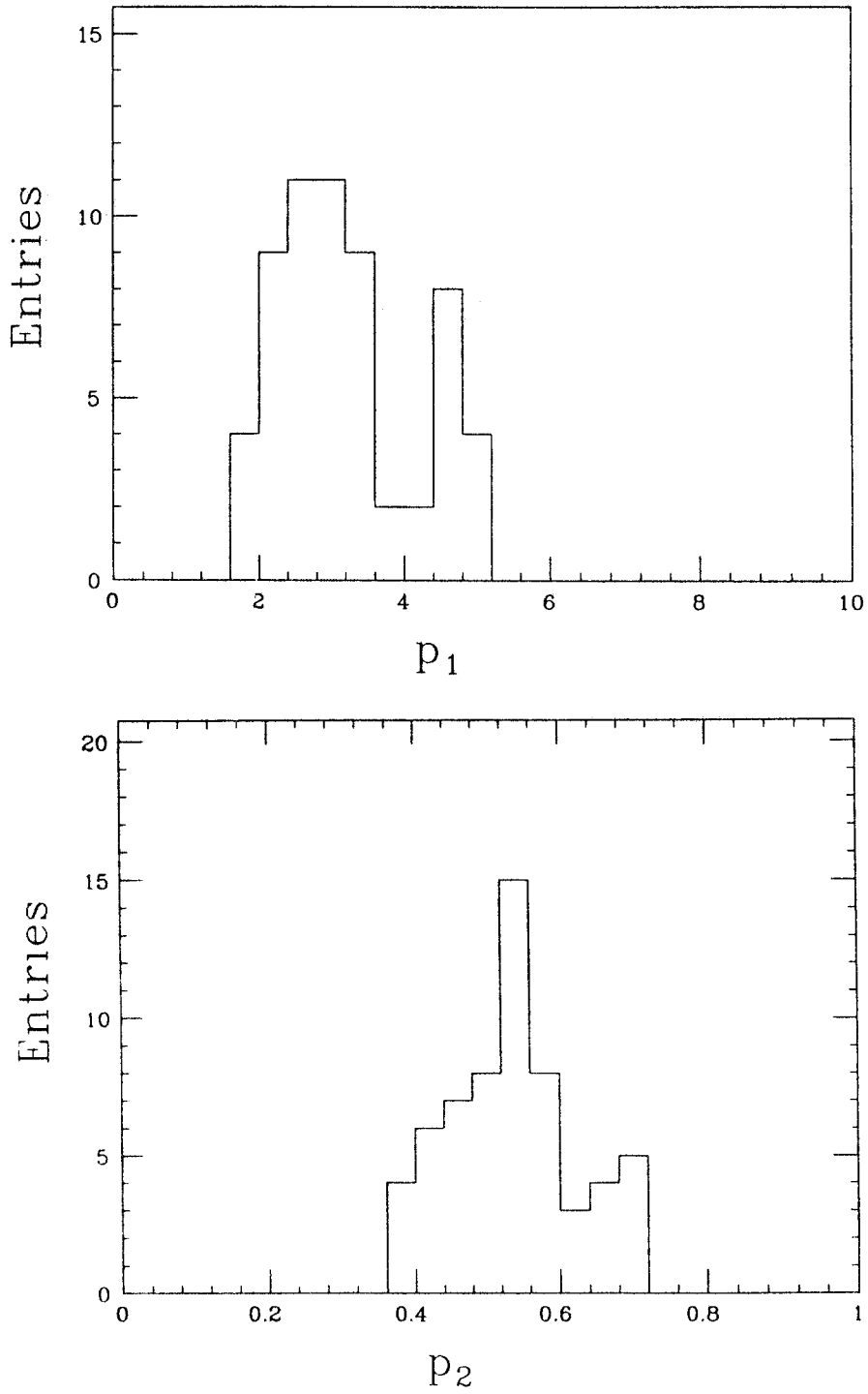

Fig. 8 Distribution of p_1 and p_2 parameters.

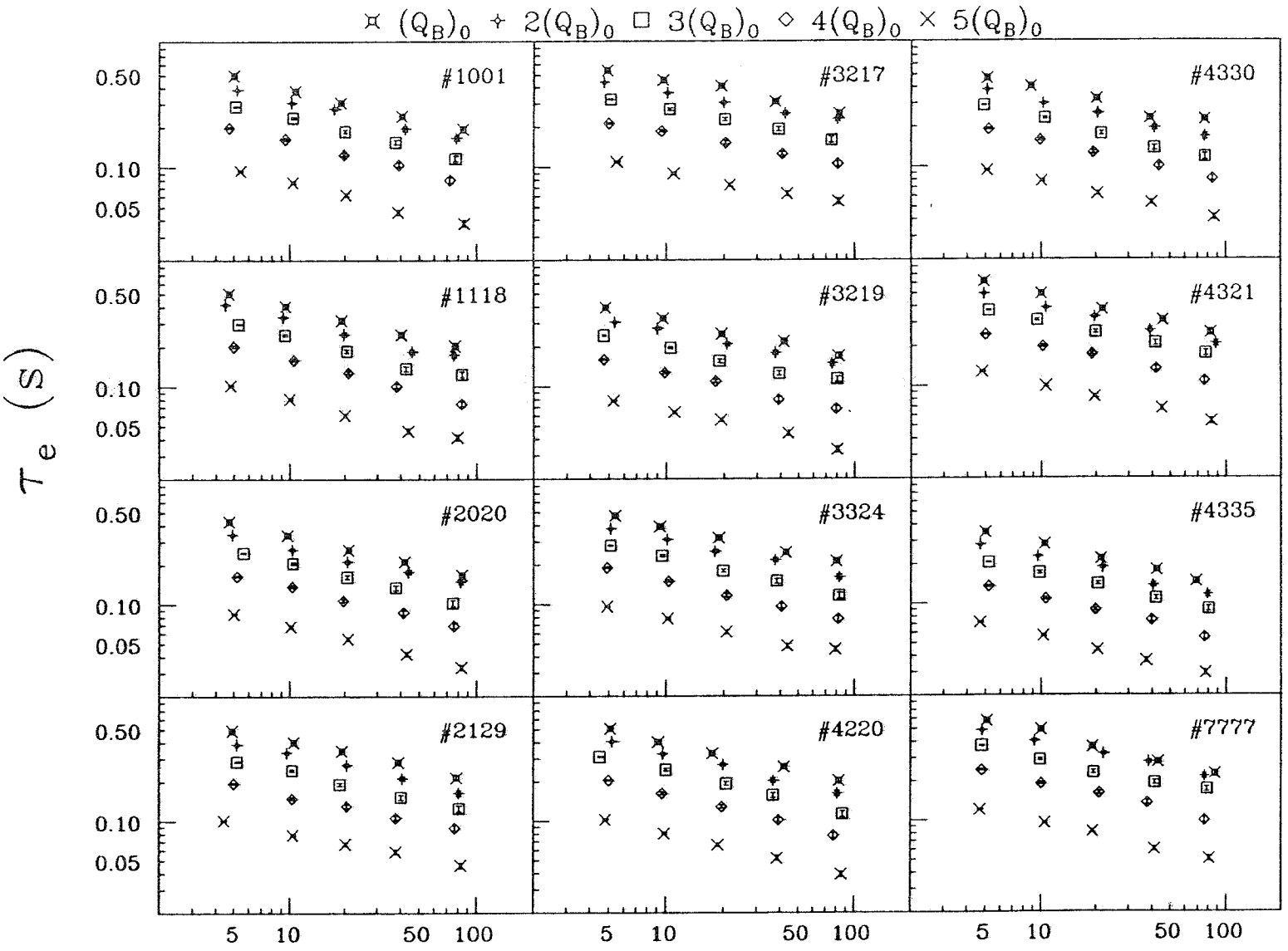

Fig. 9 Excitation times as functions of I and Q_B.

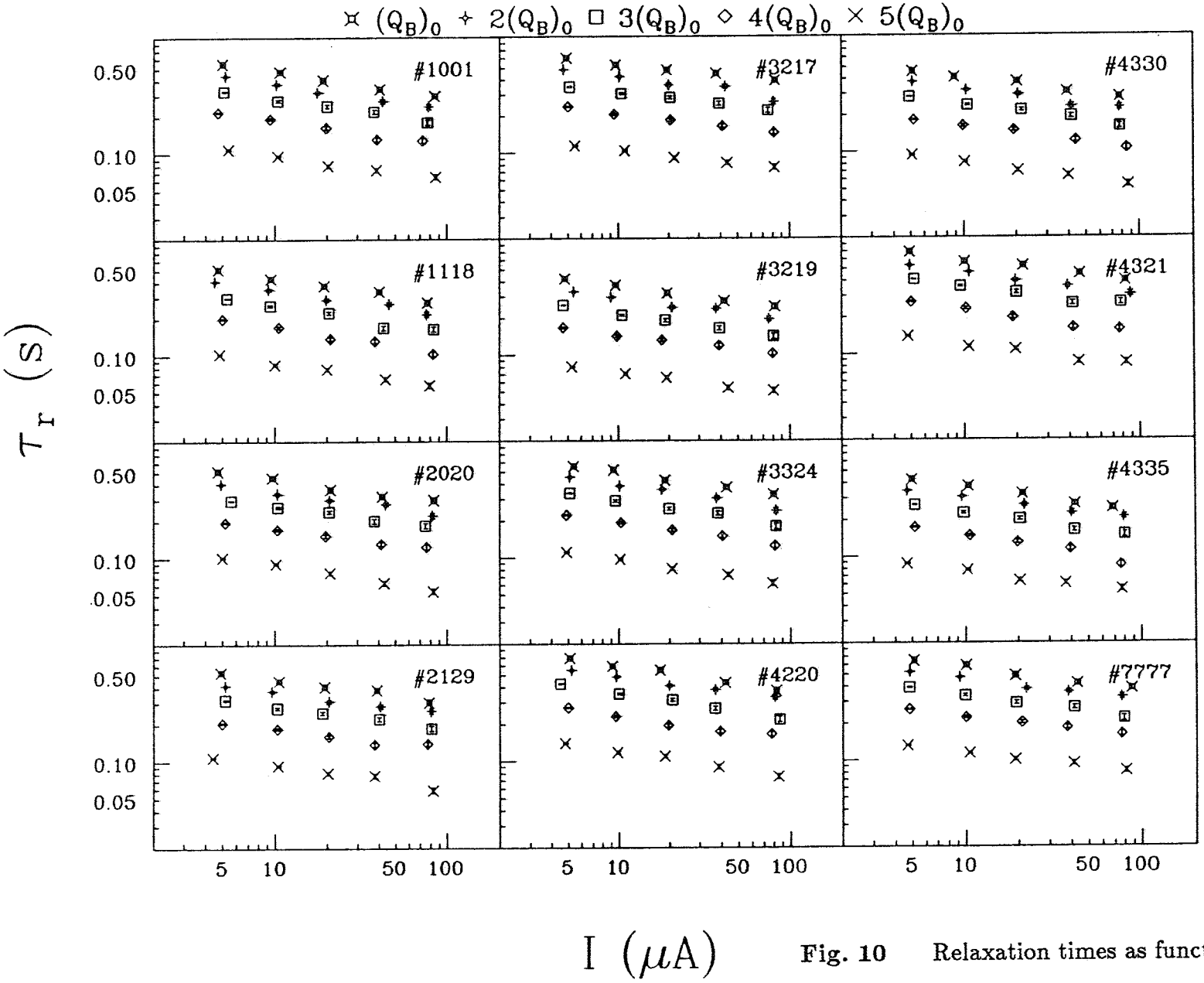

Fig. 10 Relaxation times as functions of I and Q_B.

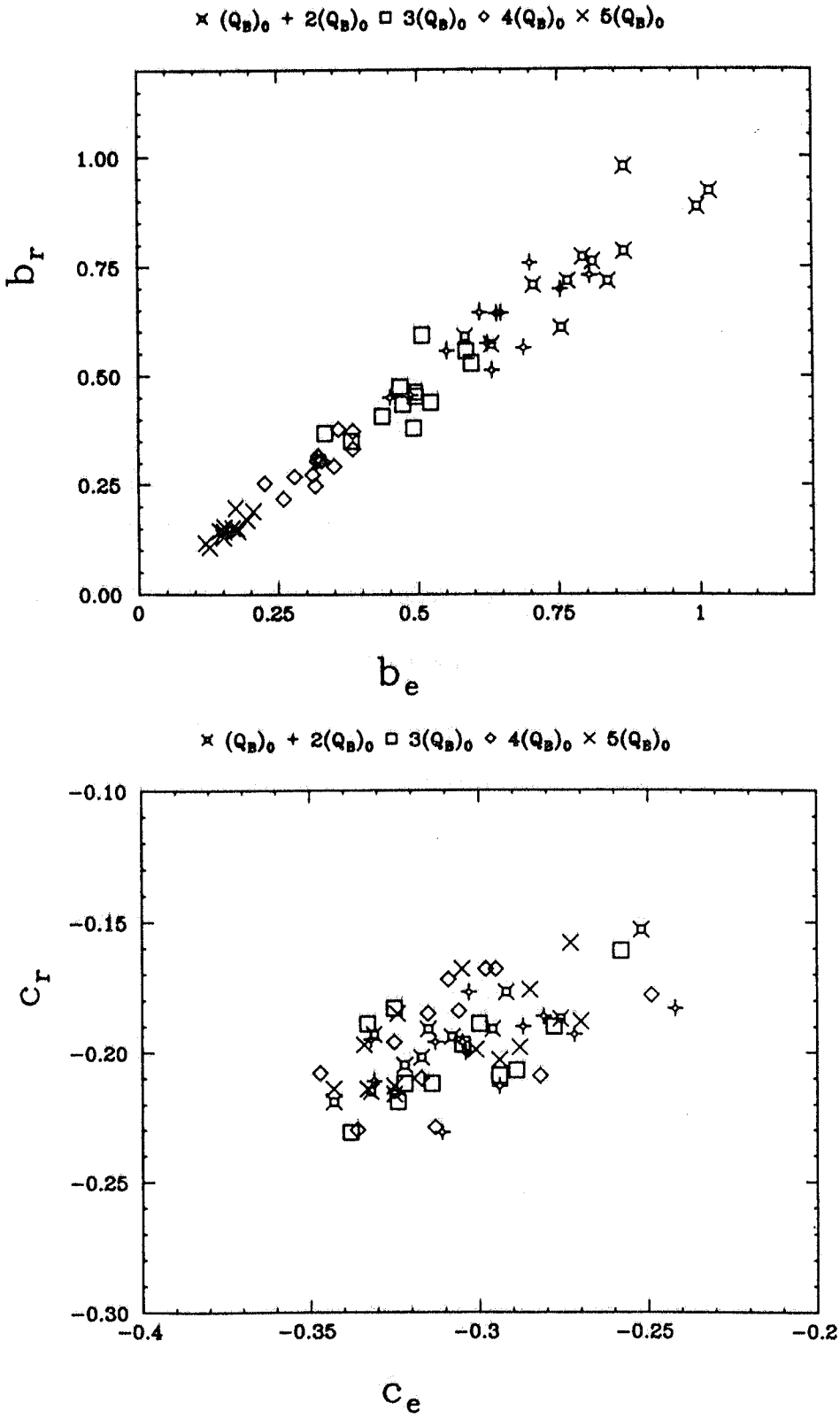

Fig. 11 Distribution of parameters $b_{e,r}$ and $c_{e,r}$, at constant HV.

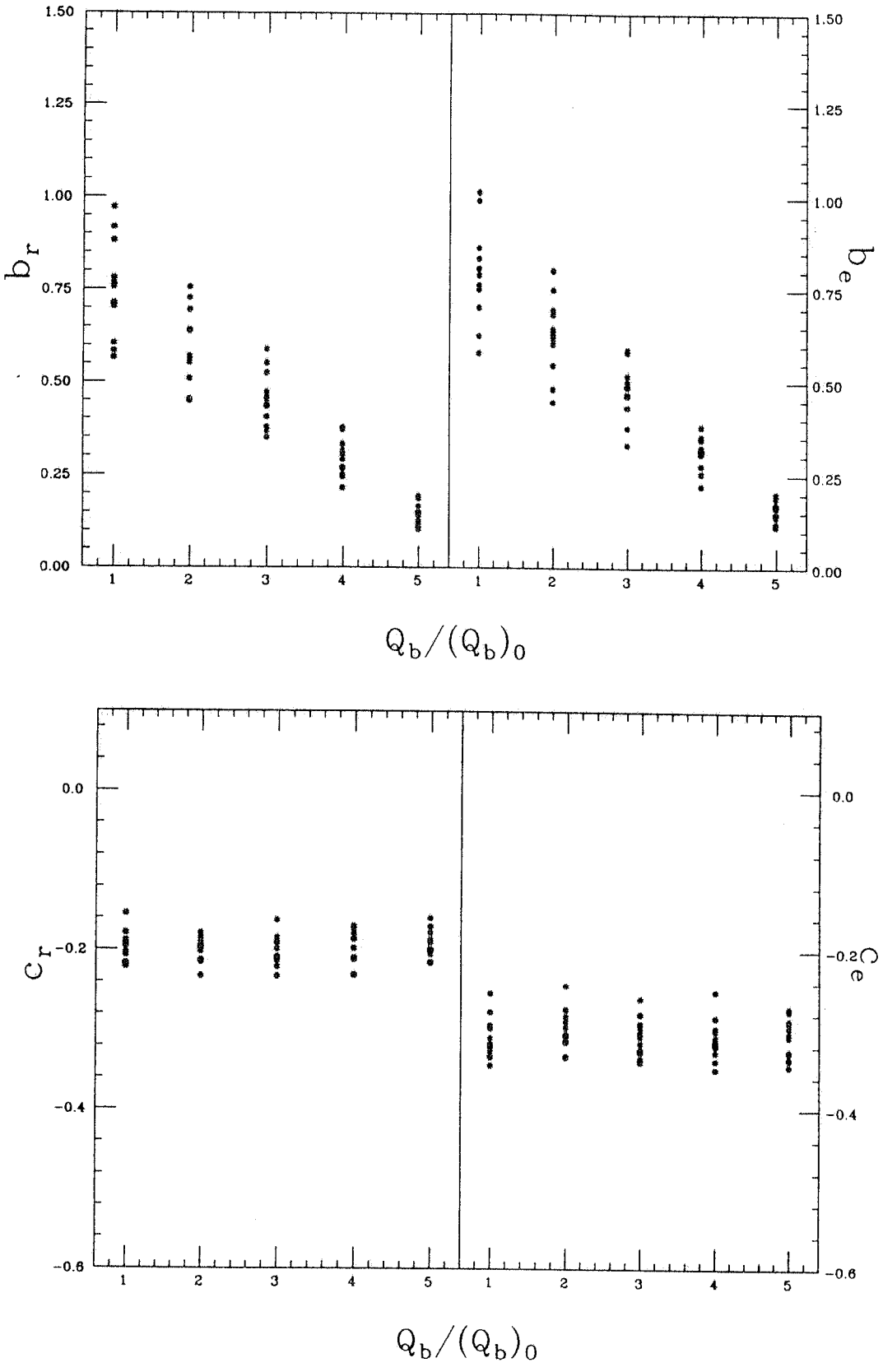

Fig. 12 Correlations between excitation and relaxation parameters $b_{e,r}$ and $c_{e,r}$, at constant HV.

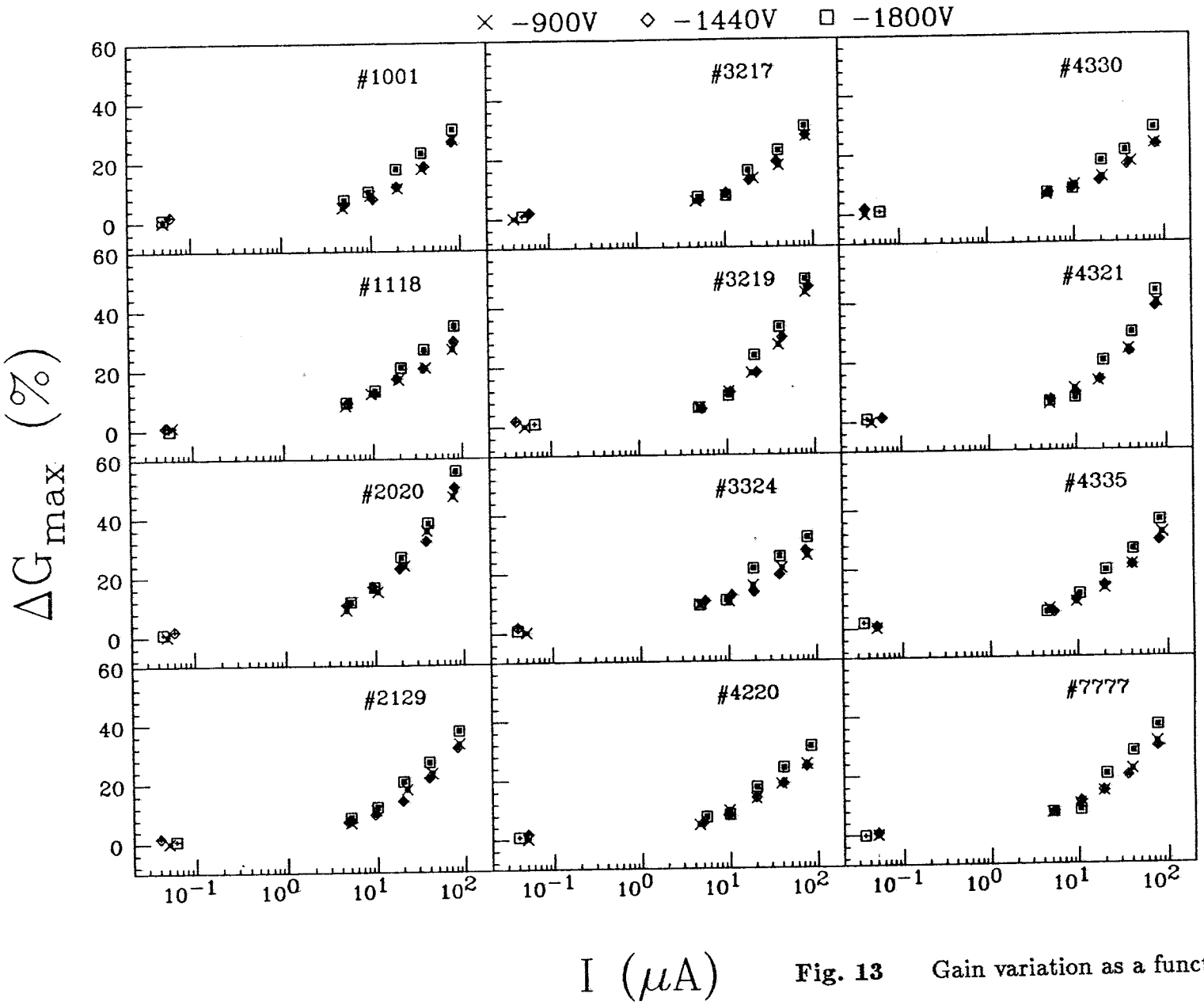

Fig. 13 Gain variation as a function of I and HV.

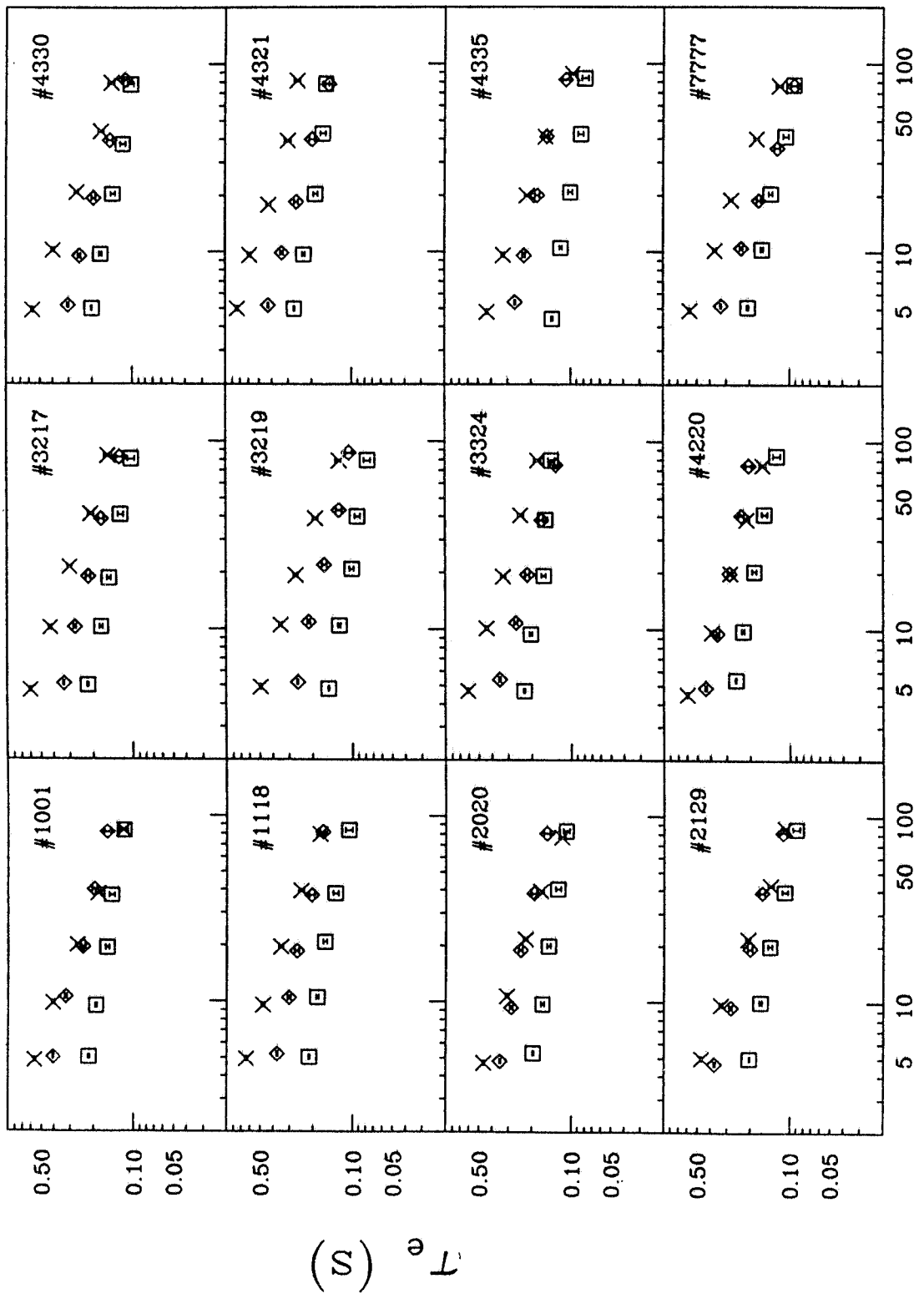

Fig. 14 Excitation times as functions of I and HV.

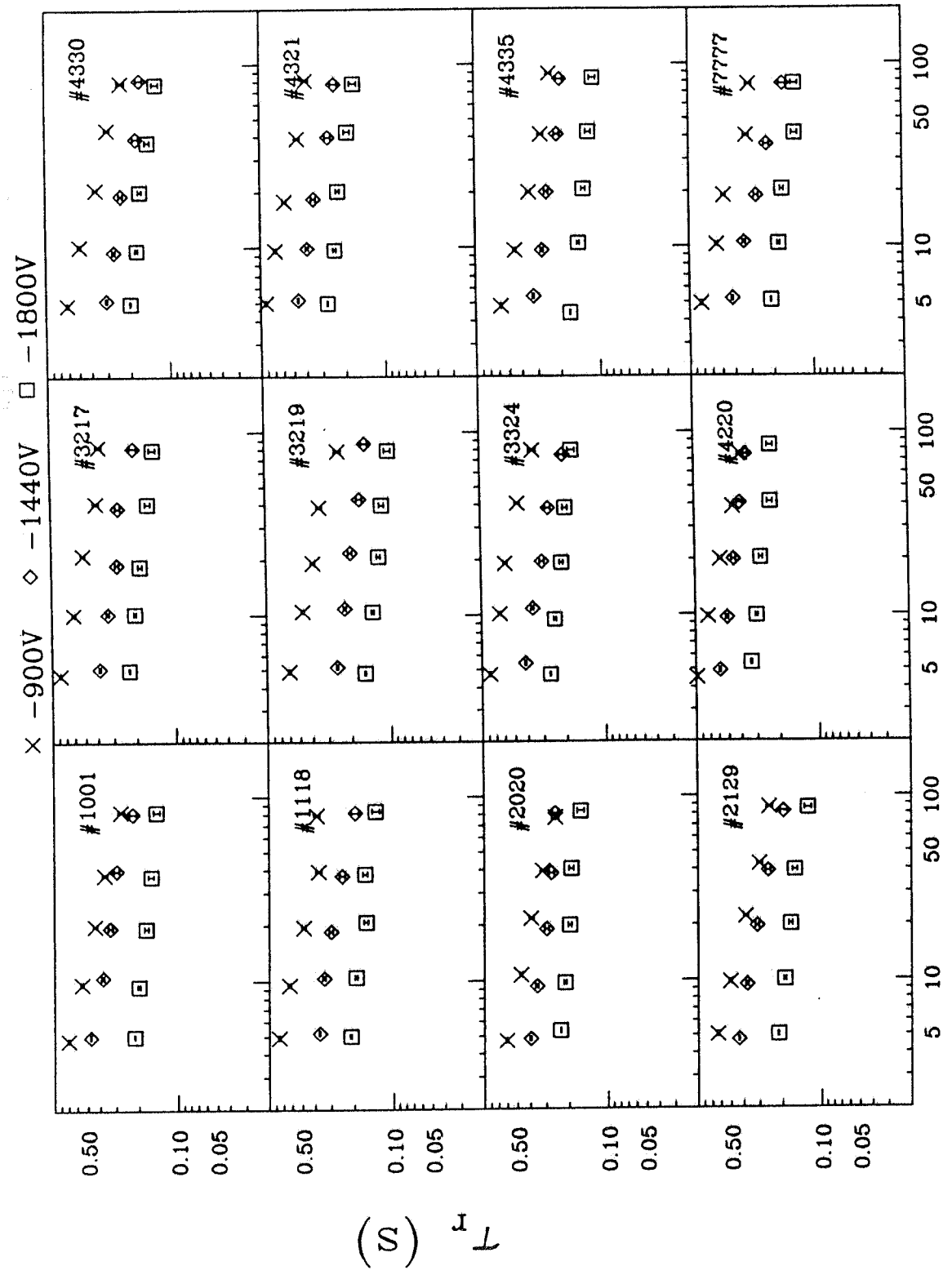

Fig. 15 Relaxation times as functions of I and HV.

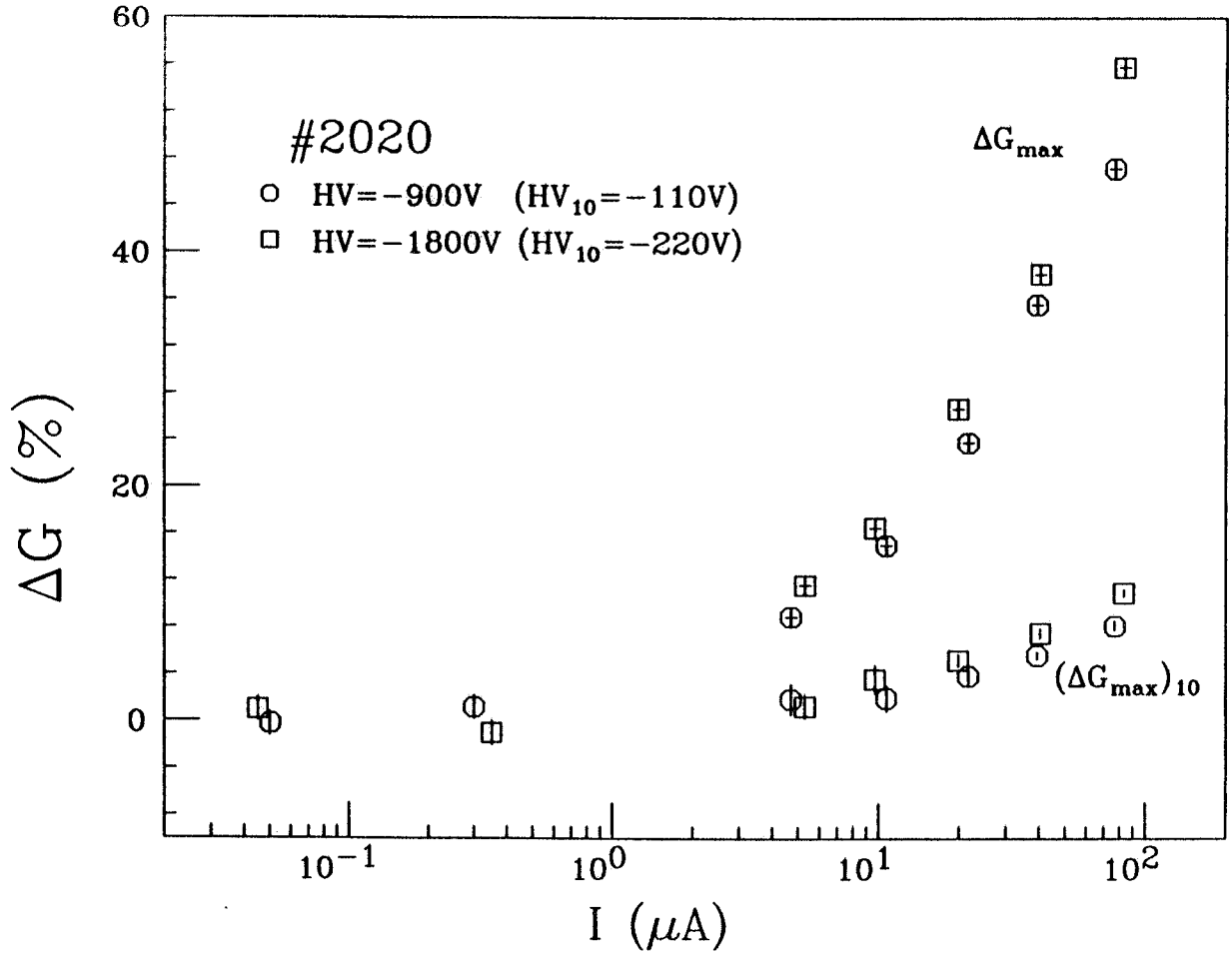

Fig. 16 The contribution of the last dynode $(\Delta G_{max})_{10}$ to the overall gain variation ΔG_{max}. Measurements have been repeated for two values of the 10th multiplicative stage voltage drop.